

CATALYTIC EFFECTS OF FE- AND CA-BASED ADDITIVES ON GAS EVOLUTION DURING PYROLYSIS OF DACHENGZI OIL SHALE OF CHINA

SHA WANG^{(a)*}, LIZHI SONG^(a), XIUMIN JIANG^(b)

^(a) Institute of Thermal Energy and Power Engineering, College of Mechanical Engineering, Shanghai University of Engineering Science, Shanghai, 201620, PR China

^(b) Institute of Thermal Energy Engineering, School of Mechanical Engineering, Shanghai Jiao Tong University, Shanghai, 200240, PR China

Abstract. The pyrolysis of Dachengzi oil shale (OS), Huadian City, China, was carried out in a stainless-steel cylindrical retort at 520 °C both in the absence and presence of catalyst under argon atmosphere to evaluate the catalytic effects of Fe_2O_3 and $CaCO_3$ additives on the products yield and characteristics of non-condensable gases. The results showed that the catalyst significantly affected the reactivity of OS kerogen pyrolysis. The shale oil yield increased after adding the catalyst, especially Fe_2O_3 , but the shale char yield decreased in the presence of the catalyst. The non-condensable gases yield rose in the $CaCO_3$ -catalysed pyrolysis and declined upon the Fe_2O_3 -catalysed process, indicating that $CaCO_3$ had a more pronounced catalytic effect on the secondary reactions of oil vapors. In addition, the gaseous products obtained both with and without the catalyst had a higher volume content of CO_2 , CH_4 and H_2 , and a lower volume content of CO and C_2 – C_4 hydrocarbons. The peak concentrations of CO_2 and H_2 increased in the presence of the catalyst, especially Fe_2O_3 , while that of CO enhanced with addition of $CaCO_3$ as a catalyst. H_2 was generated at higher temperature compared to CO_2 and CO . Furthermore, Fe_2O_3 and $CaCO_3$ exhibited different effects on the evolution of C_1 – C_4 hydrocarbons. COS and H_2S evolved almost simultaneously, the amount of H_2S released being higher than that of COS . The peak concentrations of the said gases decreased with adding the catalyst, especially Fe_2O_3 . The non-condensable gases produced both before and after catalysis mainly consisted of CO_2 and CH_4 , and some minor gases, in terms of mass distribution. The mass contents of ethane, butane, CO_2 and H_2 increased after the use of the catalyst, while those of butane, H_2S and COS decreased. Moreover, adding Fe_2O_3 and $CaCO_3$ resulted in the decline in the ethene/ethane and propene/propane ratios, respectively, suggesting that different catalysts possibly led to different changes in the physical structure of oil shale and then caused the secondary reactions of pyrolysis products to proceed to different extents.

* Corresponding author: e-mail wangsha@sues.edu.cn

CaCO₃ was more efficient than Fe₂O₃ in producing non-condensable gases of high heating value.

Keywords: *oil shale pyrolysis, catalyst, products yield, non-condensable gases, physical characteristics.*

1. Introduction

Oil shale, one kind of unconventional oil and gas resources, is a fine-grained sedimentary rock containing a large amount of kerogen which can be converted into shale oil, combustible gases and shale char through retorting processes [1, 2]. The obtained gaseous products have relatively high energy values and therefore can be used as potential fuels [3] whose yields and characteristics depend on several factors, such as the properties and component composition of oil shale, retorting temperature, heating rate, catalysts, reactor type, etc. [4–6]. For producing gas products with high yield and quality, it is necessary to investigate the characteristics of their evolution under different retorting conditions.

So far, investigators mainly focused on the evolution kinetics and distribution of various gas species produced during the non-catalytic pyrolysis of oil shale under different retorting conditions. Campbell et al. [7, 8] determined the kinetics of evolution of light gases (CO₂, CO, H₂, CH₄, and the C₂ and C₃ hydrocarbons) and their content distribution during pyrolysis of Colorado oil shale at different temperatures and heating rates. Huss and Burnham [9] measured the rates of evolution of light gases at different temperatures. Marshall et al. [10] reported the generation kinetics of key components (CO₂, H₂O and CH₄) during Australian oil shale decomposition. Charlesworth [11] described the kinetics of evolution of lower molecular weight hydrocarbons. The results indicated that the alkene to alkane ratio was dependent on the heating rate, pyrolysis temperature, type of oil shale, and, to a lesser extent, degree of conversion. All these parameters have been used as indicators of oil shale retorting conditions and may be related to secondary cracking and coking reactions of oil vapors. Wong et al. [12] determined 10 sulfur-containing pyrolysis gases ranging in concentration from several percent to less than 1 ppm produced from the pyrolysis of oil shale by using a fully computer automated triple quadrupole mass spectrometer. Reynolds et al. [13] demonstrated that the formation of non-hydrocarbon gases, particularly H₂S, CO₂, CO and H₂O, was highly dependent upon the interaction between the mineral matrix and kerogen of the shale.

On the other hand, there have been reported a few studies on the yield distribution of gas products released during the catalytic pyrolysis of oil shale. The commonly used catalysts in the pyrolysis of oil shale mainly include alkali, alkaline earth metals and transition metal species as well as their compounds [14]. Some researchers reflected that alkali and alkaline earth metal cations might affect the reactivity of oil shale pyrolysis.

Karabakan and Yürüm [15] suggested that adding calcium-based catalysts during oil shale pyrolysis was helpful for the cracking of oxygen-containing functional groups in oil shale. Also, the said catalysts could effectively remove CO₂ and gas-phase sulfur-containing compounds, such as H₂S, COS, thiophene, different sulfides and mercaptans [16–18]. Moreover, the transition metal iron is considered to be a catalyst with high catalytic activity for hydrogenation and dehydrogenation reactions. Bakr et al. [19] revealed that adding pyrite accelerated the formation of free radicals during the thermal degradation of kerogen, which, according to Gai et al. [20], might be attributed to the nascent sulfur produced during the conversion process of pyrite to pyrrhotite. Hascakir et al. [21] and Hascakir and Akin [22] put forward that adding three different iron powders (Fe, Fe₂O₃ and FeCl₃) could improve the thermal conductivity of oil shale to accomplish efficient temperature distribution and decrease the viscosity of oil by increasing the temperature, which favoured the recovery of oil from oil shale. Meanwhile, there was also shown that Fe₂O₃ had a positive effect on the breakdown of organic fuels [23]. In addition, Jiang et al. [24] proposed that the transition metal Co ion could also act as the activation center to accelerate the breakdown of chemical bonds in oil shale organic matter, and the Co ion could increase the selectivity of aromatic hydrocarbons and promote olefin aromatization. Williams and Chishti [25, 26] developed a two-stage oil shale pyrolysis reactor incorporating a second batch reactor using a zeolite ZSM-5 catalyst. Based on the experiment results obtained the researchers suggested that the gas products mainly included CO₂, CO, H₂, CH₄, C₂H₄, C₂H₆, C₃H₆ and C₃H₈, and some minor hydrocarbon gases whose concentrations after the catalysed process significantly increased compared to the products from the uncatalysed pyrolysis. It has been found that adding inexpensive, effective and environment-friendly calcium- and iron-based catalysts during the pyrolysis of oil shale may improve the process reactivity and affect the products distribution. So it is necessary to investigate the mechanism of evolution of gas products with time in the catalytic pyrolysis of oil shale.

In this paper, the low-temperature retorting of oil shale samples obtained from Dachengzi mine in Huadian City of China was carried out in a stainless retort at 520 °C in the absence and presence of the catalyst (Fe₂O₃ and CaCO₃). The effect of the catalysts on the concentrations of the gaseous products was investigated. For determining the concentrations of major non-hydrocarbon gases (CO and CO₂), C₁–C₄ hydrocarbons and sulfur-containing gases, a multi-component Fourier transform infrared (FTIR) gas analyzer GASMET DX-4000 was used. The concentrations of H₂ and CO₂ were determined employing an MRU-Vario Plus industrial portable flue gas analyzer, while the H₂S concentration was determined using a domestic EC-440 H₂S analyzer. Information about the products yields is needed not only to understand the pyrolysis reaction mechanism, but also to optimize the retorting conditions to obtain gas products of high yield and quality.

2. Experimental

2.1. Raw material and catalysts

The oil shale samples investigated in this paper were obtained from Dachengzi mine located in Huadian City, China. The general characteristics of the samples are given in Table. The original oil shale samples were crushed and screened to a mean particle size of less than 3 mm, following the National Standard of China GB 474-1996. All the samples were dried at 105 °C to constant weight and then stored in a desiccator. The choice of catalysts for the study proceeded from scientific, technical and economic considerations. The selected CaCO₃ and Fe₂O₃ were named Ca-based and Fe-based catalyst, respectively. During the experiments, the catalysts were mechanically mixed with oil shale and their mass content was 10% of the oil shale mass.

Table. Proximate and ultimate analysis of Dachengzi oil shale, wt%, ar [27, 28]

Proximate analysis		Ultimate analysis	
Moisture	11.54	C	27.33
Volatile matter	36.21	H	3.59
Ash	48.24	O ^a	7.89
Fixed carbon	4.01	N	0.57
Lower heating value, kJ/kg	11076.07	S	0.84

Note: ^a – calculated by difference; ar – as received.

2.2. Experimental setup and procedure

All experiments were performed in a stainless-steel cylindrical retort (70 mm i.d., 100 mm height), as shown in Figure 1.

The temperature of the reactor vessel was measured by a thermocouple and controlled by a proportional-integral-derivative (PID) controller. To study the effect of the catalyst on product characteristics, 50 g of the dried oil shale sample and the mixture of 50 g of the dried oil shale sample and 5 g of the catalyst were respectively fed into the reactor electrically heated at a heating rate of 12 °C min⁻¹ from room temperature to 520 °C and held for 20 minutes under argon atmosphere. The volatile products escaped from the reactor were cooled using cold traps which were immersed in low-temperature troughs (about 0 °C) filled with the mixture of ice and water. The liquid product was separated from gases, and, based on their density difference, further divided into shale oil and water in another separation unit. The gas products were sampled into the online gas analyzers. The mass of shale char and liquid product was determined, while the non-condensable gases yield was calculated by overall material balance. In this study, all the experiments were repeated twice and the product yields were calculated by an average value of two equivalent tests.

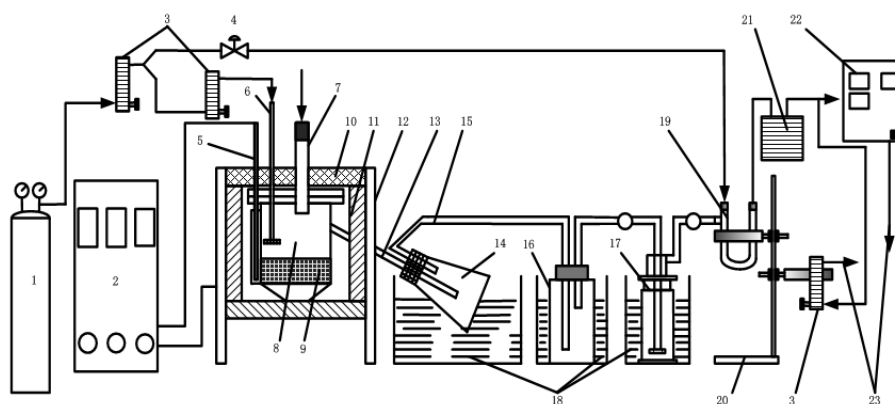


Fig. 1. Schematic diagram of the experimental oil shale retorting system.

1 – argon cylinder, 2 – automatic temperature controller, 3 – flowmeter, 4 – flow control valve, 5 – thermocouple, 6 – gas inlet, 7 – sample inlet, 8 – retort reactor, 9 – oil shale, 10 – insulation, 11 – electric heater, 12 – steel stand, 13 – copper tube, 14 – conical flask, 15 – silicone tube, 16 – wide mouthed bottle, 17 – gas washing bottle, 18 – water/ice condenser, 19 – U-tube, 20 – stand, 21 – gas flowmeter, 22 – gas analyzer, 23 – vent.

2.3. Gas analysis

For analysis the gas products were sampled into the online gas analyzers. A multi-component FTIR gas analyzer GASMET DX-4000 was used to analyze major non-hydrocarbon gases (CO and CO_2), C_1 – C_4 hydrocarbons and sulfur-containing gases. H_2 and CO_2 were subjected to analysis by employing an MRU-Vario Plus industrial portable flue gas analyzer, while a domestic EC-440 H_2S analyzer was used for analyzing H_2S . The heating value of non-condensable gases is the sum of heating values of effective gas components.

3. Results and discussion

3.1. Product yield

Figure 2 shows the average yields of shale char, shale oil, non-condensable gases and water produced by retorting oil shale in the absence and presence of the catalyst at $520\text{ }^\circ\text{C}$ with a heating rate of $12\text{ }^\circ\text{C min}^{-1}$ under argon atmosphere. The product yield presented in the figure refers to the weight ratio of the derived product to raw oil shale sample.

It can be seen from Figure 2 that the shale char yield slightly decreases in the presence of Fe_2O_3 and CaCO_3 as catalysts, being respectively 67.49 and 67.18 wt%. The volatile matter content increases after the addition of the catalyst, especially CaCO_3 . In addition, the figure displays that after adding Fe_2O_3 and CaCO_3 the shale oil yield is respectively 1.02 and 1.01 times that

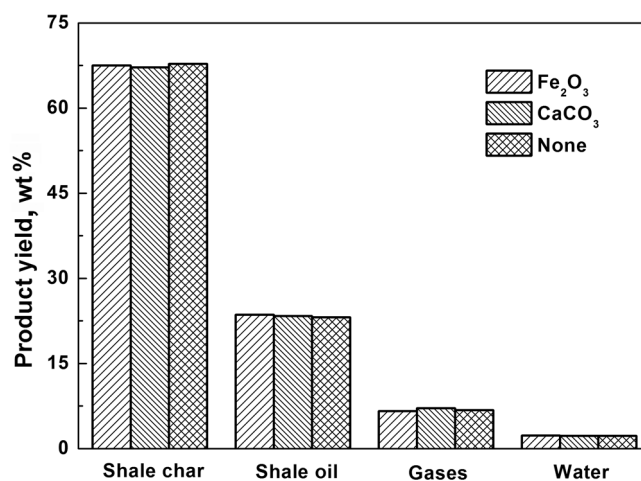


Fig. 2. Influence of different catalysts on the yield of products derived by retorting Dachengzi oil shale.

obtained in the non-catalytic retorting process, and the non-condensable gases yield is respectively 97% and 1.05 times that obtained in the absence of the catalyst. The catalytic behavior of different catalysts in the pyrolysis of oil shale is possibly related to their different catalytic mechanisms. The alkali and alkaline earth metal carbonates have a positive effect on the cracking of oxygen-containing functional groups in oil shale. At the same time, the alkaline earth metal cations may react with $-\text{COOH}$ and $-\text{OH}$ functional groups to form the alkaline earth-oxygen complexes or clusters [29]. Meanwhile, it has also been reported that Fe_2O_3 can reduce the bond energy of oxygen-containing functional groups and mainly react with $-\text{COOH}$ and $\text{C}-\text{OH}$ to generate iron-oxygen complexes or clusters [30, 31]. These complexes probably serve as the active sites on the oil shale sample surface, resulting in a significant increase of the reactivity of oil shale pyrolysis. So it is observed that the shale char yield decreases and the shale oil yield increases after adding the catalyst. In addition, iron as a transition element exhibits high catalytic activity in hydrogenation and dehydrogenation reactions, in which there are involved unpaired d-orbital electrons and a vacant orbital of low energy. The active metal iron atoms will easily attract hydrogen molecules to form chemisorption bonds when the hydrogen molecules are close enough to the active surface of the metal catalyst. Then the hydrogen molecules can decompose to active hydrogen atoms which will react with free radicals fragments or olefins formed during oil shale pyrolysis to produce stable low-molecular-weight oil [23]. Simultaneously, Hascakir et al. [21] and Hascakir and Akin [22] indicated that adding Fe_2O_3 into an electrically heating retort could improve the thermal conductivity of oil shale samples to accomplish efficient temperature distribution. In addition, Fe_2O_3 enhances the reaction rate by decreasing the activity energy of the pyrolysis

reaction, and also reduces the viscosity of oil, causing the oil gas to rapidly evolve from the reactor, which results in the increase of shale oil yield after the addition of the catalyst. Rizkiana et al. [32] also suggested that Fe could transfer the heat more effectively since generally it has higher thermal conductivity. The oil shale could be rapidly heated and thus the pyrolysis would take place more intensely during a very short time. Therefore, the shale oil yield is much higher from the Fe_2O_3 -catalysed pyrolysis compared to that obtained after adding CaCO_3 .

On the other hand, the addition of the catalyst probably results in the change of the physical structure of oil shale particles during the pyrolysis process [33]. Qi et al. [34] also reported that the pore structure of char changed significantly during the catalytic pyrolysis of coal. In this work, the non-condensable gas yield after the addition of CaCO_3 was higher compared to that obtained after adding Fe_2O_3 , indicating that the said catalysts might have a different influence on the structure of oil shale particles in the pyrolysis process. The different physical structure of oil shale particles may cause the oil gas to evolve from them at different times and lead to the secondary reactions of oil vapors in the particles to different extents. The secondary reactions of oil vapors are more vigorous after the use of CaCO_3 .

3.2. Concentration distribution of non-condensable gases

The non-condensable gases generated from retorting oil shale mainly comprise some non-hydrocarbon gases (CO_2 , CO and H_2) and small molecule hydrocarbon gases (C_1 – C_4 alkanes and C_2 – C_4 alkenes). The volume percentages of these gases obtained in the presence and absence of the catalyst in relation to reaction time are shown in Figures 3–6.

As can be seen from Figures 3–6, the amounts of CO_2 , CH_4 and H_2 obtained are high and those of CO and C_2 – C_4 hydrocarbon gases are low. In addition, Figure 3a shows that CO_2 begins to evolve at 290 °C, while its amount evolved gradually increases with rising temperature and reaches the peak value at 490–500 °C. The peak concentration of CO_2 increases after the addition of the catalyst, the increase being especially remarkable after adding Fe_2O_3 . CO_2 is a common product of the thermal treatment of organic matter, while its high amounts are typically produced upon the generation of hydrocarbons from the thermal cracking of kerogen, probably due to decarboxylation of organic acids and esters. At the initial stage of oil shale pyrolysis, CO_2 is mainly produced by decarboxylation of carboxyl groups. When the temperature rises up to 400–530 °C, the aliphatic and aromatic C–H bonds and oxygen-containing functional groups, e.g. carboxyl groups, in oil shale are broken. The carboxyl groups firstly decompose to form CO and then CO combines with oxygen atoms in oil shale to produce CO_2 . So the peak concentration of CO_2 is mainly observed in this temperature range [35].

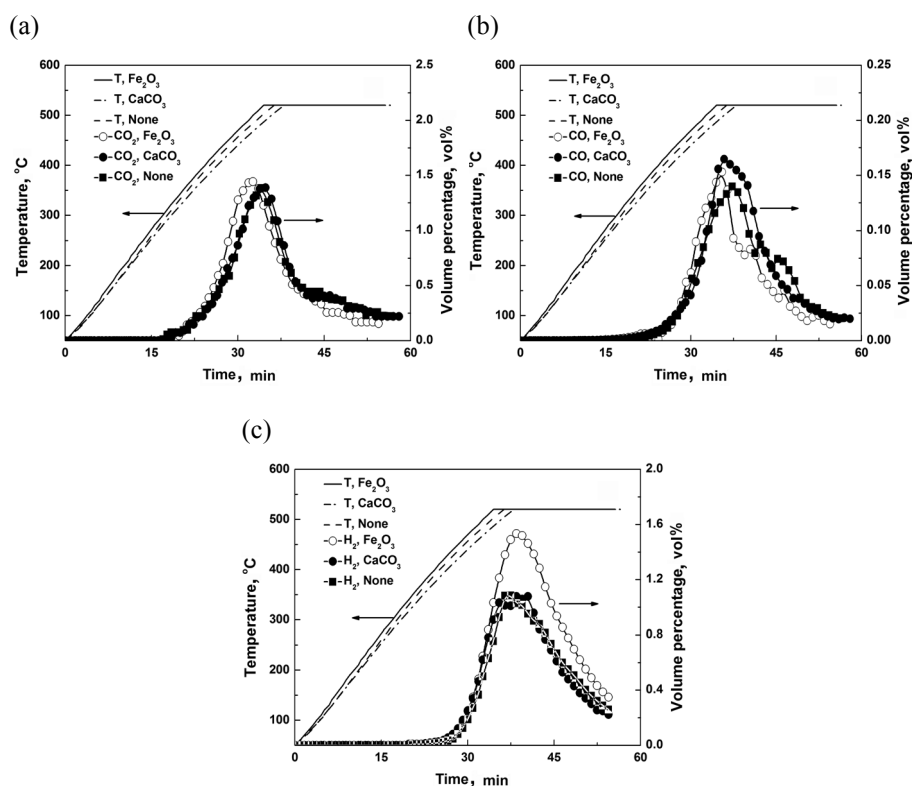


Fig. 3. Volume percentages of non-hydrocarbon gases obtained from oil shale pyrolysis in the presence of different catalysts as a function of reaction time.

Figure 3b demonstrates that CO begins to evolve at about 310 °C and 290 °C respectively in the absence and presence of the catalyst. As the temperature increases, the CO concentration goes up and reaches the maximum value at 500–520 °C in the absence of the catalyst. The peak concentration of CO is increased by adding the catalyst, the increase being more noticeable after adding CaCO₃. The above suggests that the two catalysts favour the formation of CO. CO released during oil shale pyrolysis may result from the cleavage of organic oxygen-containing functional groups in oil shale, such as –COOH, –OH, –COH, etc. The phenolic hydroxyl groups, ether bonds and carbonyl groups decompose to generate CO. The carbonyl groups are broken to generate CO at about 400 °C, and the heteroaryl epoxy is broken to produce CO at higher temperature [36].

Figure 3c shows that H₂ begins to be released at about 340 °C. The H₂ evolution temperature is higher than those of CO and CO₂, which is possibly because less hydrogen is generated as oil shale earlier decomposes to bitumen. The H₂ concentration increases with increasing temperature and reaches the maximum value after staying constant for 1–2 min at 520 °C. The peak concentration of H₂ rises after the addition of the catalyst and

increases more noticeably under the catalytic action of Fe_2O_3 , which gives evidence of that Fe_2O_3 and CaCO_3 have a catalytic effect on the formation of hydrogen, while Fe_2O_3 exhibits a much higher catalytic activity. In the pyrolysis process, trace amounts of H_2 are generated as kerogen decomposes to form bitumen, and a high amount of H_2 is produced during the pyrolysis of bitumen, which mainly results from the dehydrogenation of the side chains of aromatics, alkanes and cycloalkanes [8].

Figures 4 and 5 show the evolution of methane and $\text{C}_2\text{--C}_4$ hydrocarbons to occur at about 380°C and $420\text{--}440^\circ\text{C}$, respectively. The concentrations of $\text{C}_1\text{--C}_4$ hydrocarbons reach the maximum value after staying constant for a few minutes at 520°C , and exhibit different trends of change after the addition of the catalyst. Generally, the methane evolved during the oil shale pyrolysis process may result primarily from the cleavage of methyl and methoxyl groups attached to aromatic and aliphatic structures, as well as the cleavage of methylene bridges connecting the aromatic rings. In addition, methane is mostly produced by the secondary reactions of compounds that have already been released by the thermal decomposition of kerogen. The $\text{C}_2\text{--C}_4$ hydrocarbons are mainly generated from the cleavage of aliphatic side

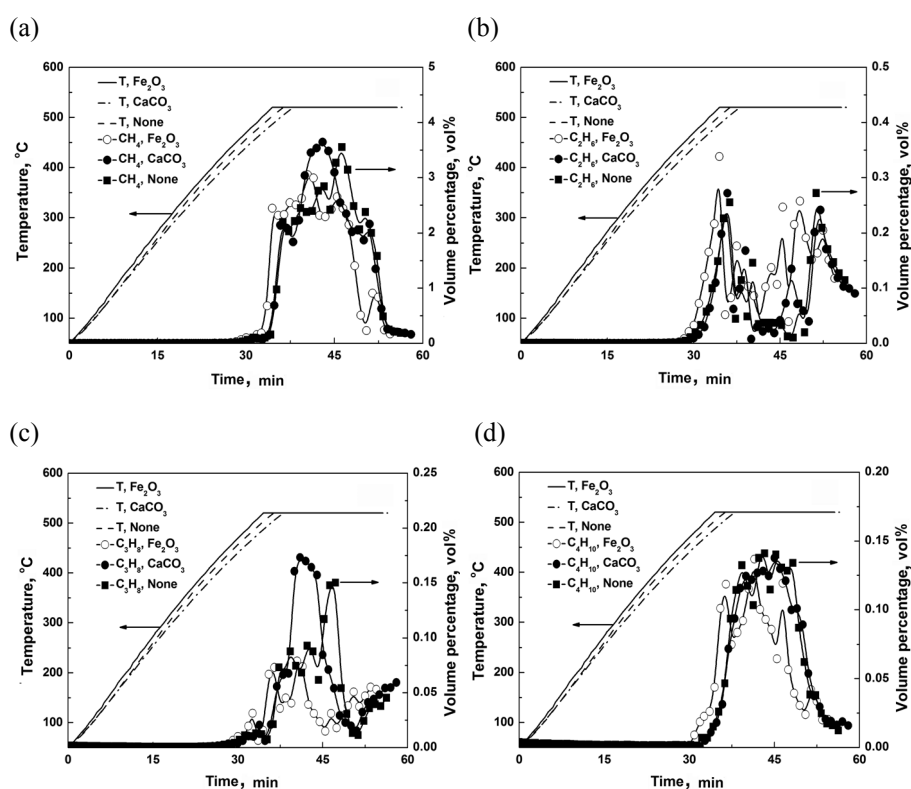


Fig. 4. Volume percentages of alkane gases obtained in the presence of different catalysts as a function of reaction time.

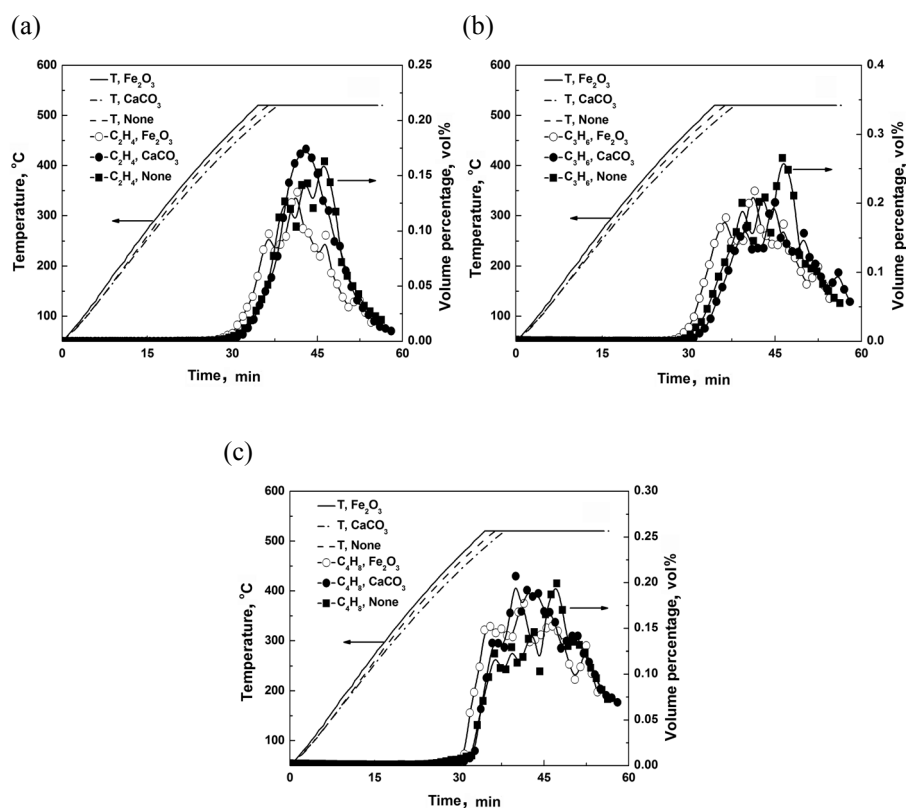


Fig. 5. Volume percentages of alkene gases obtained in the presence of different catalysts as a function of reaction time.

chains attached to the aromatic structures and formed from cracking of aliphatic hydrocarbons via free radical mechanisms [37]. These reactions can be enhanced by adding the catalyst, which results in the increase of the content of H₂ and decrease of that of some hydrocarbons.

Figure 6 reveals that the non-condensable gases also include the sulfur-containing compounds COS and H₂S. Both the products are released in the pyrolysis process of oil shale with and without the catalyst, the content of H₂S being higher. H₂S evolves at about 300 °C. Its concentration increases with rising temperature and reaches the maximum value after staying constant for less than 4 min at 520 °C. Moreover, the peak concentration of COS occurs at 480–490 °C. The two gases are nearly simultaneously released. H₂S and COS are possibly produced by the decomposition of pyrite and organic sulfur in oil shale, while COS may originate from the reaction between CO and pyrite or sulfur derived from the decomposition of pyrite. The concentrations of H₂S and COS are affected by the pyrolysis atmosphere and secondary reactions. As the H₂ concentration in the gaseous products

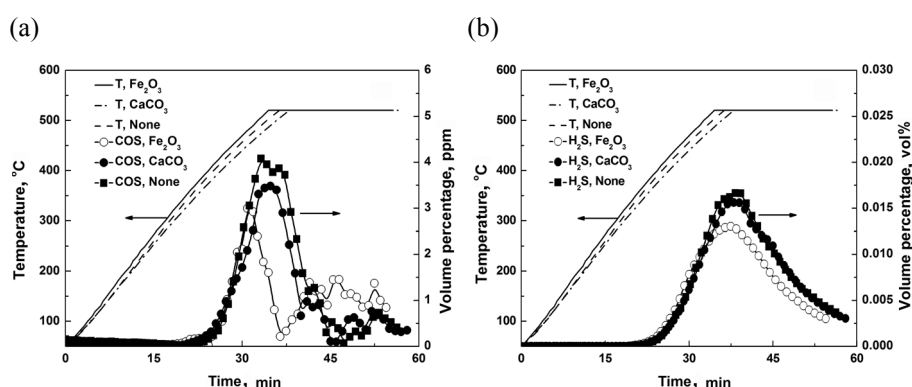


Fig. 6. Volume percentages of sulfur-containing gases obtained in the presence of different catalysts as a function of reaction time.

increases, the extent of COS evolution may be limited by the shift reaction $\text{COS} + \text{H}_2 = \text{CO} + \text{H}_2\text{S}$, however, this reaction promotes the generation of H_2S . Adding the catalyst has only a slight impact on the concentration of H_2S and COS in the initial stage of their generation, while the peak concentrations of the gases are affected to a greater extent. So, the peak concentrations of H_2S and COS decrease after the addition of the catalyst, and drop more abruptly after adding Fe_2O_3 . It is possibly because adding CaCO_3 may lead to the following reactions: $\text{H}_2\text{S} + \text{CaCO}_3 = \text{CaS} + \text{H}_2\text{O} + \text{CO}_2$ and $\text{COS} + \text{CaCO}_3 = \text{CaS} + 2\text{CO}_2$ [38]. CO_2 and H_2O generated in the two reactions will react with pyrite in oil shale to generate H_2S and COS. And, after adding Fe_2O_3 to oil shale by mechanically mixing, the catalyst is mainly adhered to the external surface of oil shale particles and reacts with the sulfur-containing gases generated by pyrolysis of oil shale to form metal sulfide when they diffuse from the interior of oil shale particles to their surface. The optimal sulfidation temperature of iron-based sorbents is 450–550 °C [39]. In this temperature range, the H_2S concentration significantly decreases and the metal sulfide Fe_{1-x}S produced may react with CO_2 in the pyrolysis gas products: $\text{Fe}_{1-x}\text{S} + \text{CO}_2 = \text{Fe}_{1-x}\text{O} + \text{COS}$. So the decrease of COS concentration is less marked than that of H_2S in the Fe_2O_3 -catalysed pyrolysis process.

3.3. Mass distribution and heating value of non-condensable gases

The mass distribution of non-condensable gases is calculated by the volume percentage shown in Figures 3–6 and the volume flow rate of the gases. The heating value of non-condensable gases is the sum of low heating values of effective gas components. The mass distribution and heating value of non-condensable gases produced in the absence and presence of the catalyst are depicted in Figure 7.

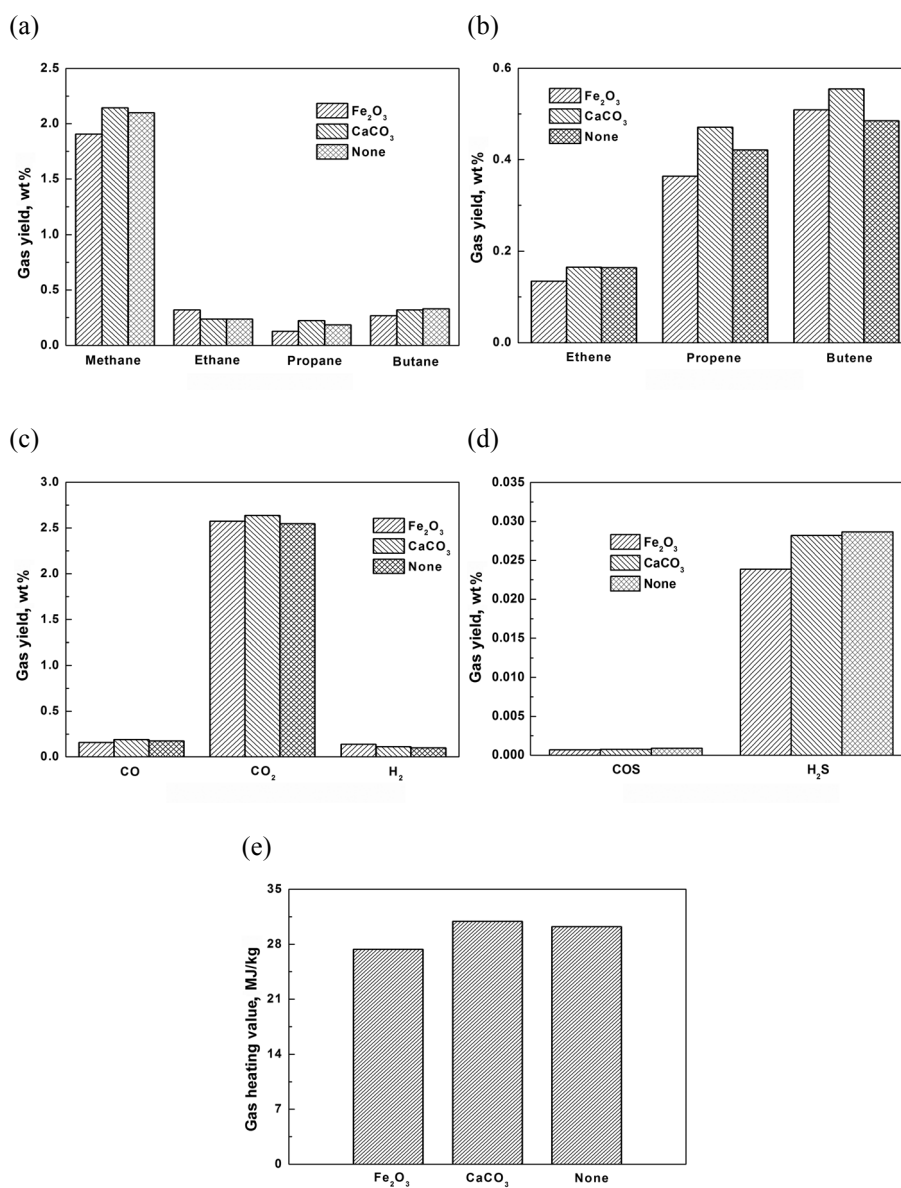


Fig. 7. Influence of different catalysts on the composition and heating value of non-condensable gases: (a) alkane gases; (b) alkene gases; (c) non-hydrocarbon gases; (d) sulfur-containing gases; (e) heating value of non-condensable gases.

As can be seen from Figure 7, the gases obtained from the pyrolysis of oil shale mainly consist of CO_2 and CH_4 , and some minor gases. Adding Fe_2O_3 increases the mass contents of ethane, butane, CO_2 and H_2 and decreases those of H_2S , COS and other hydrocarbons, while the mass contents of all

the gases except butane, H₂S and COS increase after adding CaCO₃. The overall yield of non-condensable gases increases in the presence of CaCO₃ possibly because its effect on the secondary reactions of oil vapors is more pronounced than that of Fe₂O₃.

In addition, based on Figures 7a and 7b, the ethene/ethane, propene/propane, butene/butane and total alkene/alkane ratios in the absence and presence of the catalyst can be obtained. The alkene/alkane ratio has been used to determine the reaction mechanism and characterize pyrolysis conditions. For example, Williams and Ahmad [4] and Carter and Taulbee [40] suggested that the increase in the ethene/ethane, propene/propane, butene/butane and total alkene/alkane ratios with increasing temperature might be related to the acceleration of the secondary gas phase cracking reaction. As Figures 7a and 7b show, after adding Fe₂O₃, the ethene/ethane ratio drops from 0.69 to 0.42, while those of propene/propane, butene/butane and total alkene/alkane increase from 2.29 to 2.90, 1.48 to 1.90 and 0.376 to 0.384, respectively. Meanwhile, after the addition of CaCO₃, the propene/propane ratio decreases from 2.29 to 2.11, while the ethene/ethane, butene/butane and total alkene/alkane ratios increase from 0.69 to 0.70, 1.48 to 1.74 and 0.376 to 0.408, respectively. Jacobson et al. [41] also reported that the ethene/ethane ratio could be used as the indicator of oil shale retorting conditions, in particular pyrolysis temperature. Raley [42] presented a chemical reaction mechanism to explain the oil vapor cracking reactions, and found that the declined oil yield was related to the increased ethene/ethane ratio. Williams and Nazzal [43] considered that the ethene/ethane, propene/propane, butene/butane and total alkene/alkane ratios increased with rising pyrolysis temperature, reflecting the acceleration of secondary reactions and increase of aromatics concentration of shale oil. This work demonstrates that the butene/butane and total alkene/alkane ratios increase after the addition of the catalyst, but the ethene/ethane and propene/propane ratios exhibit different trends of change. This suggests that the two catalysts may exert a different effect on the structural changes of oil shale in the pyrolysis process as well as on the secondary reactions of the pyrolysis products.

Figure 7e displays that the heating value of non-condensable gases is 30.209, 27.349 and 30.913 MJ/kg without the catalyst and in the presence of Fe₂O₃ and CaCO₃, respectively, which indicates that CaCO₃ is more efficient than Fe₂O₃ in producing non-condensable gases of high heating value.

4. Conclusions

In this paper, the gas evolution characteristics were investigated in the absence and presence of catalysts, Fe₂O₃ and CaCO₃. Based on the results obtained, the following conclusions were drawn:

1. After the addition of the catalyst, the shale oil yield increases and the shale char yield decreases. More shale oil is produced in the presence of

Fe₂O₃ compared to CaCO₃. The non-condensable gases yield rises in the CaCO₃-catalysed pyrolysis and declines in the presence of Fe₂O₃. The results indicate that adding the catalyst affects the reactivity of kerogen pyrolysis and the secondary reactions of oil vapors. In addition, the catalysts exert a different effect on the oil shale pyrolysis due to different catalytic mechanisms.

2. The volume percentages of CO₂, CH₄ and H₂ in the non-condensable gases produced are much higher and those of CO and C₂–C₄ hydrocarbons are lower. The peak concentrations of CO₂ and H₂ increase after adding the catalyst, especially Fe₂O₃, while that of CO also increases in the presence of especially CaCO₃. Fe₂O₃ and CaCO₃ have a different impact on the evolution of C₁–C₄ hydrocarbons. COS and H₂S evolve nearly simultaneously, the H₂S content being higher than that of COS. The catalyst has a low effect on the concentrations of H₂S and COS in the initial stage of their evolution, while the influence on the gases peak concentrations is higher. The peak concentrations of H₂S and COS decrease after adding the catalyst, especially Fe₂O₃.
3. The produced non-condensable gases mainly consist of CO₂ and CH₄, as well as some minor gases, in terms of mass distribution. After the use of the catalyst, the mass contents of ethane, butane, CO₂ and H₂ increase, while those of butane, H₂S and COS decrease. The total non-condensable gases yield increases after adding CaCO₃, indicating that this compound has a more pronounced catalytic effect on the secondary reactions of oil vapors. Adding Fe₂O₃ and CaCO₃ respectively reduces the ethane/ethane and propene/propane ratios, suggesting that different catalysts have a different impact on the changes in the structure of oil shale and therefore cause the secondary reactions of pyrolysis products to proceed at different rates. CaCO₃ is more efficient than Fe₂O₃ in producing non-condensable gases of high heating value.

Acknowledgements

The authors express their gratitude to the State Key Laboratory of Heavy Oil Processing of China University of Petroleum for carrying out the shale oil samples analysis and giving technical advice. This work was supported by the National Natural Science Foundation of China (Grants No. 50906051 and No. 51704194), the Young Teacher Training Scheme of Shanghai Universities (Grant No. ZZGCD15062) and the Research Start-up Fund of Shanghai University of Engineering Science (Grant No. 2015-52).

REFERENCES

1. Wang, S., Jiang, X. M., Han, X. X., Tong, J. H. Effect of retorting temperature on product yield and characteristics of non-condensable gases and shale oil obtained by retorting Huadian oil shales. *Fuel Process. Technol.*, 2014, **121**, 9–15.

2. Na, J. G., Im, C. H., Chung, S. H., Lee, K. B. Effect of oil shale retorting temperature on shale oil yield and properties. *Fuel*, 2012, **95**, 131–135.
3. Tiwari, P., Deo, M. Compositional and kinetic analysis of oil shale pyrolysis using TGA–MS. *Fuel*, 2012, **94**, 333–341.
4. Williams, P. T., Ahmad, N. Influence of process conditions on the pyrolysis of Pakistani oil shales. *Fuel*, 1999, **78**(6), 653–662.
5. Al-Harashseh, A., Al-Ayed, O., Al-Harashseh, M., Abu-El-Halawah, R. A. Heating rate effect on fractional yield and composition of oil retorted from El-lajjun oil shale. *J. Anal. Appl. Pyrol.*, 2010, **89**(2), 239–243.
6. Nazzal, J. M. The influence of grain size on the products yield and shale oil composition from the Pyrolysis of Sultani oil shale. *Energ. Convers. Manage.*, 2008, **49**(11), 3278–3286.
7. Campbell, J. H., Koskinas, G. J., Gallegos, G., Gregg, M. Gas evolution during oil shale pyrolysis. 1: Nonisothermal rate measurements. *Fuel*, 1980, **59**(10), 718–726.
8. Campbell, J. H., Gallegos, G., Gregg, M. Gas evolution during oil shale pyrolysis. 2. Kinetic and stoichiometric analysis. *Fuel*, 1980, **59**(10), 727–732.
9. Huss, E. B., Burnham, A. K. Gas evolution during pyrolysis of various Colorado oil shales. *Fuel*, 1982, **61**(12), 1188–1196.
10. Marshall, C. P., Kannangara, G. S. K., Wilson, M. A., Guerbois, J.-P., Hartung-Kagi, B., Hart, G. Potential of thermogravimetric analysis coupled with mass spectrometry for the evaluation of kerogen in source rocks. *Chem. Geol.*, 2002, **184**(3–4), 185–194.
11. Charlesworth, J. M. Oil shale pyrolysis. 2. Kinetics and mechanism of hydrocarbon evolution. *Ind. Eng. Chem. Proc. Des. Dev.*, 1985, **24**(4), 1125–1132.
12. Wong, C. M., Crawford, R. W., Burnham, A. K. Determination of sulfur-containing gases from oil shale pyrolysis by triple quadrupole mass spectrometry. *Anal. Chem.*, 1984, **56**(3), 390–395.
13. Reynolds, J. G., Crawford, R. W., Burnham, A. K. Analysis of oil shale and petroleum source rock pyrolysis by triple quadrupole mass spectrometry: comparisons of gas evolution at the heating rate of 10 °C/min. *Energ. Fuel.*, 1991, **5**(3), 507–523.
14. Abbasi-Atibeh, E., Yozgatligil, A. A study on the effects of catalysts on pyrolysis and combustion characteristics of Turkish lignite in oxy-fuel conditions. *Fuel*, 2014, **115**, 841–849.
15. Karabakan, A., Yürüm, Y. Effect of the mineral matrix in the reactions of oil shales: 1. Pyrolysis reactions of Turkish Göynük and US Green River oil shales. *Fuel*, 1998, **77**(12), 1303–1309.
16. Sadiki, A., Kaminsky, W., Halim, H., Bekri, O. Fluidised bed pyrolysis of Moroccan oil shales using the hamburg pyrolysis process. *J. Anal. Appl. Pyrol.*, 2003, **70**(2), 427–435.
17. Floess, J. K., Plawsky, J., Longwell, J. P., Peters, W. A. Effects of calcined dolomite on the fluidized bed pyrolysis of a Colorado oil shale and a Texas lignite. *Ind. Eng. Chem. Proc. Des. Dev.*, 1985, **24**(3), 730–737.
18. Ellig, D. L., Lai, C. K., Mead, D. W., Longwell, J. P., Peters, W. A. Pyrolysis of volatile aromatic hydrocarbons and n-heptane over calcium oxide and quartz. *Ind. Eng. Chem. Proc. Des. Dev.*, 1985, **24**(4), 1080–1087.
19. Bakr, M. Y., Yokono, T., Sanada, Y., Akiyama, M. Role of pyrite during the thermal degradation of kerogen using in situ high-temperature ESR technique. *Energ. Fuel.*, 1991, **5**(3), 441–444.

20. Gai, R. H., Jin, L. J., Zhang, J. B., Wang, J. Y., Hu, H. Q. Effect of inherent and additional pyrite on the pyrolysis behavior of oil shale. *J. Anal. Appl. Pyrol.*, 2014, **105**, 342–347.
21. Hascakir, B., Babadagli, T., Akin, S. Experimental and numerical simulation of oil recovery from oil shales by electrical heating. *Energ. Fuel.*, 2008, **22**(6), 3976–3985.
22. Hascakir, B., Akin, S. Recovery of Turkish oil shales by electromagnetic heating and determination of the dielectric properties of oil shales by an analytical method. *Energ. Fuel.*, 2010, **24**(1), 503–509.
23. Feng, J., Xue, X. Y., Li, X. H., Li, W. Y., Guo, X. F., Liu, K. Products analysis of Shendong long-flame coal hydrolysis with iron-based catalysts. *Fuel Process. Technol.*, 2015, **130**, 96–100.
24. Jiang, H. F., Song, L. H., Cheng, Z. Q., Chen, J., Zhang, L., Zhang, M. Y., Hu, M. J., Li, J. N., Li, J. F. Influence of pyrolysis condition and transition metal salt on the product yield and characterization via Huadian oil shale pyrolysis. *J. Anal. Appl. Pyrol.*, 2015, **112**, 230–236.
25. Williams, P. T., Chishti, H. M. Two stage pyrolysis of oil shale using a zeolite catalyst. *J. Anal. Appl. Pyrol.*, 2000, **55**(2), 217–234.
26. Williams, P. T., Chishti, H. M. Influence of residence time and catalyst regeneration on the pyrolysis–zeolite catalysis of oil shale. *J. Anal. Appl. Pyrol.*, 2001, **60**(2), 187–203.
27. Han, X. X., Jiang, X. M., Cui, Z. G. Studies of the effect of retorting factors on the yield of shale oil for a new comprehensive utilization technology of oil shale. *Appl. Energ.*, 2009, **86**(11), 2381–2385.
28. Li, S. Q., Yao, Q., Chi, Y., Yan, J. H., Cen, K. F. Pilot-scale pyrolysis of scrap tires in a continuous rotary kiln reactor. *Ind. Eng. Chem. Res.*, 2004, **43**(17), 5133–5145.
29. Liu, Q. R., Hu, H. Q., Zhou, Q., Zhu, S. W., Chen, G. H. Effect of inorganic matter on reactivity and kinetics of coal pyrolysis. *Fuel*, 2004, **83**(6), 713–718.
30. Fu, Y., Guo, Y. H., Zhang, K. X. Effect of three different catalysts (KCl, CaO, and Fe₂O₃) on the reactivity and mechanism of low-rank coal pyrolysis. *Energ. Fuel.*, 2016, **30**(3), 2428–2433.
31. William, L. H., Michel, B. Transition metal and metal oxide catalysed gasification of carbon by oxygen, water, and carbon dioxide. *Fuel*, 1983, **62**(2), 132–165.
32. Rizkiana, J., Guan, G. Q., Widayatno, W. B., Hao, X. G., Wang, Z. D., Zhang, Z. L., Abudula, A. Oil production from mild pyrolysis of low-rank coal in molten salts media. *Appl. Energ.*, 2015, **154**, 944–950.
33. Jiang, H. F., Song, L. H., Cheng, Z. Q., Chen, J., Zhang, L., Zhang, M. Y., Hu, M. J., Li, J. N., Li, J. F. Influence of pyrolysis condition and transition metal salt on the product yield and characterization via Huadian oil shale pyrolysis. *J. Anal. Appl. Pyrol.*, 2015, **112**, 230–236.
34. Qi, X. J., Guo, X., Xue, L. C., Zheng, C. G. Effect of iron on Shenfu coal char structure and its influence on gasification reactivity. *J. Anal. Appl. Pyrolysis*, 2014, **110**, 401–407.
35. Yu, H. L., Jiang, X. M. Study of pyrolysis property of Huadian oil shale. *Journal of Fuel Chemistry and Technology*, 2001, **29**(5), 450–455 (in Chinese).
36. Qin, Z. *Effect of Iron and Potassium Additives on Transformation of Sulfur and Pyrolysis Characteristics of Coal*. Master Dissertation, Taiyuan University of Technology, 2012 (in Chinese).

37. Artok, L., Schobert, H. H. Reaction of carboxylic acids under coal liquefaction conditions. 2: Under hydrogen atmosphere. *J. Anal. Appl. Pyrol.*, 2000, **54**(1–2), 235–246.
38. Guan, R. G., Li, W., Li, B. Q. Effects of Ca-based additives on pyrolysis of Datong coal. *Journal of China University of Mining & Technology*, 2002, **31**(4), 396–401.
39. Ren, X. R. *Desulfurization Performance of Iron Manganese Based Sorbents at Mid-Temperature and Effect of Ambient Gases on Them*. Doctoral Dissertation, Taiyuan University of Technology, 2010 (in Chinese).
40. Carter, S. D., Taulbee, D. N. Fluidized bed steam retorting of Kentucky oil shale. *Fuel Processing Technology*, 1985, **11**(3), 251–272.
41. Jacobson, I. A., Decora, A. W., Cook, G. L. Retorting indexes for oil shale pyrolysis from ethane/ethane ratios of product gases. In: *Science and Technology of Oil Shale* (Yen, T. F. ed.). Ann Arbor Science Publishers, Ann Arbor, MI, 1976, p. 103.
42. Raley, J. H. Monitoring oil shale retorts by off-gas alkene/alkane ratios. *Fuel*, 1980, **59**(6), 419–424.
43. Williams, P. T., Nazzari, J. M. Polycyclic aromatic compounds in oils derived from the fluidised bed pyrolysis of oil shale. *J. Anal. Appl. Pyrol.*, 1995, **35**(2), 181–197.

Presented by J. Soone

Received October 11, 2016